



A theoretical liquid crystal elastomer model that mimics the elasticity of cat skin

L. Angela Mihai¹

Received: 30 March 2023 / Accepted: 25 April 2023 / Published online: 15 June 2023
© The Author(s) 2023

Abstract

A mathematical model for nematic liquid crystal elastomers is proposed that mimics the elastic response of cat skin where reorientation of dermal fibres produces an increase in the thickness direction under tensile stretch. To capture this unusual effect, the uniaxial order parameter in the nematic elastomer model is allowed to decrease then increase again, and the critical stretch at which this change of monotonicity occurs and where the director also rotates suddenly is predicted. In addition, the model parameters are described by probability density functions and their uncertainty is propagated numerically to the predicted mechanical results.

Keywords Liquid crystal elastomer · Large strain elasticity · Auxetic response · Uncertainty quantification · Biomimetic materials · Mathematical modelling

“Of particular relevance here is the fact that technology of people must be different from that of nature simply because the two span different size scales [...] Everyday terms such as ‘assembly’, ‘polymer’, ‘blueprint’, ‘safety factor’, ‘design’, and ‘intended application’ were meant for our production systems, and we run considerable risk of self-deception when we use them for natural systems.” - S. Vogel [16]

1 Introduction

Extensive experimental programs have demonstrated the capability of a class of nematic liquid crystal elastomer (LCEs) to present certain auxetic responses, while their volume is conserved under large elastic strain [8–13]. In particular, when a material sample is stretched longitudinally, its thickness, measured in the direction perpendicular to the sample’s plane, first decreases, then increases if the deformation is sufficiently large, then decreases again. Such mechanical behaviour is generated at a molecular level, without porosity emerging at macroscopic scale, and it is accompanied by a mechanical Fréedericksz transition whereby the nematic director, which is initially aligned within the sample’s plane and perpendicular to the longitudinal direction, rotates suddenly to become parallel with the applied force.

Auxetic materials that are simple to fabricate and avoid porosity-related weakening have long been sought for applications in a range of industries including sports equipment, aerospace, biomedical materials and architecture. Because of the intrinsic similarities between LCEs and conventional rubber [17], suitable descriptions can be achieved by adapting existing hyperelastic models for rubber-like solids [5]. Hyperelastic materials are the class of material models described by a strain-energy density function with respect to a fixed reference configuration.

In [6], a quantitative model is proposed and calibrated to available experimental data for auxetic LCEs. To analyse the effect of different model parameters on the predicted mechanical response, a simplified qualitative model is developed in

✉ L. Angela Mihai
MihaiLA@cardiff.ac.uk

¹ School of Mathematics, Cardiff University, Cardiff, UK

[7]. The theoretical analysis suggests that auxeticity can be obtained by letting the uniaxial scalar order parameter decrease to a sufficiently low value then increase again. This is in agreement with the experimental observations where, in addition, mechanical biaxiality can also be observed that enhances the auxetic behaviour.

The purpose of this paper is to present a mathematical model for nematic LCEs that is capable of predicting a similar auxetic behaviour as that found in cat skin where reorientation of dermal fibres produces an increase in the thickness direction under tensile stretch. Cat skin thickening occurs first at small strain and continues at large strain until a maximum stretch is attained, after which the skin thickness begins to decrease. Both compressible and incompressible isotropic hyperelastic models are found acceptable within the range of experimental data, as reported in [15]. For the incompressible LCE model mimicking such behaviour, the uniaxial order parameter is allowed to decrease then increase again, and the critical stretch at which this change in monotonicity and where the director also rotates suddenly is predicted. In addition, a stochastic elasticity framework [5] is adopted where the model parameters are described by probability density functions, and the uncertainty in those parameters is propagated numerically to the predicted mechanical results. The theoretical model is described and explained in Section 2. This model is then calibrated to experimental data showing the auxeticity of cat skin in Section 3. The stochastic framework is summarised in the appendix.

2 Stochastic strain-energy function

In this paper, the model functions describing an incompressible nematic LCE satisfy the following assumptions [5]:

- (C1) **Objectivity (frame-indifference).** This condition states that the scalar strain-energy function is unaffected by a superimposed rigid-body transformation, which involves a change of position after deformation. As the nematic director \mathbf{n} is defined with respect to the deformed configuration, it transforms when this configuration is rotated, whereas the nematic director \mathbf{n}_0 for the reference configuration does not.
- (C2) **Isotropy.** This property requires that the strain-energy function is unaffected by a rigid-body transformation prior to deformation. As \mathbf{n} is defined with respect to the deformed configuration, it does not change when the reference configuration is rotated, whereas \mathbf{n}_0 does.

These fundamental assumptions underpin also the finite elasticity and liquid crystal theories [2, 14].

In particular, the following two-term strain-energy function is considered,

$$W^{(lce)} = \frac{\mu_1}{2n^2} (\lambda_1^{2n} + \lambda_2^{2n} + \lambda_3^{2n}) + \frac{\mu_2}{2m^2} (\alpha_1^{2m} + \alpha_2^{2m} + \alpha_3^{2m}), \quad (1)$$

where $\mu_1, \mu_2 > 0$ and m, n are given parameters, with $\mu = \mu_1 + \mu_2$ representing the shear modulus at infinitesimal strain, $\{\lambda_1^2, \lambda_2^2, \lambda_3^2\}$ denote the eigenvalues of the Cauchy-Green tensor \mathbf{FF}^T , where \mathbf{F} is the deformation gradient from the reference cross-linking state, satisfying $\det \mathbf{F} = 1$, and $\{\alpha_1^2, \alpha_2^2, \alpha_3^2\}$ are the eigenvalues of \mathbf{AA}^T , where $\mathbf{A} = \mathbf{G}^{-1}\mathbf{F}\mathbf{G}_0$ is the local elastic deformation tensor, such that $\det \mathbf{A} = 1$, with \mathbf{G}_0 and \mathbf{G} representing the ‘natural’ deformation tensors due to the liquid crystal director in the reference and current configuration, respectively.

Given an intrinsically uniaxial LCE, the natural gradient tensor takes the form [7],

$$\mathbf{G} = a^{-1/6} \mathbf{I} + (a^{1/3} - a^{-1/6}) \mathbf{n} \otimes \mathbf{n}, \quad (2)$$

where \mathbf{n} is the nematic director, \otimes denotes the tensor product of two vectors, $\mathbf{I} = \text{diag}(1, 1, 1)$ is the second order identity tensor, and

$$a = \frac{1 + 2Q}{1 - Q} \quad (3)$$

represents the anisotropy parameter, with Q the uniaxial scalar order parameter. In the reference configuration, \mathbf{G} is replaced by \mathbf{G}_0 , with \mathbf{n}_0 instead of \mathbf{n} , a_0 instead of a , and Q_0 instead of Q .

The model function defined by equation (1) can be regarded as a slight generalisation of the strain-energy density proposed in [7] where $m = -n$. Similar but more general models were introduced and analysed in [6]. In addition, here, it is assumed that the shear modulus μ follows a Gamma probability density function (see Appendix A for details), while m, n are deterministic constants.

For the LCE sample, in a Cartesian system of coordinates (X_1, X_2, X_3) , we designate the plane formed by the first two directions as the sample’s plane and the third direction as its thickness direction. The LCE is elastically deformed by

application of a tensile force in the first (longitudinal) direction, while the nematic director is initially along the second (transverse) direction.

Setting the nematic director in the reference and current configuration, respectively, as follows,

$$\mathbf{n}_0 = \begin{bmatrix} 0 \\ 1 \\ 0 \end{bmatrix}, \quad \mathbf{n} = \begin{bmatrix} \sin \theta \\ \cos \theta \\ 0 \end{bmatrix}, \tag{4}$$

where $\theta \in [0, \pi/2]$ is the angle between \mathbf{n} and \mathbf{n}_0 , the deformation gradient takes the form

$$\mathbf{F} = \text{diag} (\lambda_1, \lambda_2, \lambda_3), \tag{5}$$

such that $\det \mathbf{F} = \lambda_1 \lambda_2 \lambda_3 = 1$.

Assuming that the rotation of the nematic director within the plane formed by its initial orientation and the applied force from $\theta = 0$ to $\theta = \pi/2$ happens suddenly [6, 7], we denote by λ_{cr1} the longitudinal stretch ratio λ_1 where the rotation occurs. In practice, although the angle θ may take intermediate values between 0 and $\pi/2$, the deformation interval for which the director rotation is observed can be very short, and its separate analysis will be omitted.

When the director for the reference and current configuration are given by (4), the associated natural deformation tensors are, respectively,

$$\mathbf{G}_0 = \text{diag} (a_0^{-1/6}, a_0^{1/3}, a_0^{-1/6}) \tag{6}$$

and

$$\mathbf{G} = \begin{bmatrix} a^{-1/6} + (a^{1/3} - a^{-1/6}) \sin^2 \theta & (a^{1/3} - a^{-1/6}) \sin \theta \cos \theta & 0 \\ (a^{1/3} - a^{-1/6}) \sin \theta \cos \theta & a^{-1/6} + (a^{1/3} - a^{-1/6}) \cos^2 \theta & 0 \\ 0 & 0 & a^{-1/6} \end{bmatrix}. \tag{7}$$

The elastic deformation tensor $\mathbf{A} = \mathbf{G}^{-1} \mathbf{F} \mathbf{G}_0$ is then equal to

$$\mathbf{A} = \begin{bmatrix} \lambda_1 a_0^{-1/6} (a^{-1/3} \sin^2 \theta + a^{1/6} \cos^2 \theta) & \lambda_2 a_0^{1/3} (a^{-1/3} - a^{1/6}) \sin \theta \cos \theta & 0 \\ \lambda_1 a_0^{-1/6} (a^{-1/3} - a^{1/6}) \sin \theta \cos \theta & \lambda_2 a_0^{1/3} (a^{1/6} \sin^2 \theta + a^{-1/3} \cos^2 \theta) & 0 \\ 0 & 0 & \lambda_3 a_0^{-1/6} a^{1/6} \end{bmatrix}. \tag{8}$$

In particular:

- If $\theta = 0$, then

$$\mathbf{G} = \text{diag} (a^{-1/6}, a^{1/3}, a^{-1/6}); \tag{9}$$

- If $\theta = \pi/2$, then

$$\mathbf{G} = \text{diag} (a^{1/3}, a^{-1/6}, a^{-1/6}) \tag{10}$$

For the corresponding elastic Cauchy-Green tensor $\mathbf{A}^T \mathbf{A} = \text{diag} (\alpha_1^2, \alpha_2^2, \alpha_3^2)$, where “ T ” denotes the transpose (see also [6]), we have:

- If $\theta = 0$, then

$$\alpha_1^2 = \lambda_1^2 a_0^{-1/6} a^{1/6}, \quad \alpha_2^2 = \lambda_2^2 a_0^{1/3} a^{-1/3}, \quad \alpha_3^2 = \lambda_3^2 a_0^{-1/6} a^{1/6}; \tag{11}$$

- If $\theta = \pi/2$, then

$$\alpha_1^2 = \lambda_1^2 a_0^{-1/6} a^{-1/3}, \quad \alpha_2^2 = \lambda_2^2 a_0^{1/3} a^{1/6}, \quad \alpha_3^2 = \lambda_3^2 a_0^{-1/6} a^{1/6}. \tag{12}$$

Under the uniaxial deformation considered here, the second and third directions must be stress free. Then the corresponding principal Cauchy stresses, defined by

$$T_i^{(lce)} = \frac{\partial W^{(lce)}}{\partial \lambda_i} \lambda_i - p, \quad i = 1, 2, 3, \tag{13}$$

with p denoting the usual Lagrange multiplier for the incompressibility constraint, take the form

$$\begin{aligned} T_i^{(lce)} &= \frac{\mu_1}{n} (\lambda_i^{2n} - \lambda_2^{2n}) + \frac{\mu_2}{m} (\alpha_i^{2m} - \alpha_2^{2m}) \\ &= \frac{\mu_1}{n} (\lambda_i^{2n} - \lambda_3^{2n}) + \frac{\mu_2}{m} (\alpha_i^{2m} - \alpha_3^{2m}), \quad i = 1, 2, 3. \end{aligned} \tag{14}$$

The associated first Piola-Kirchhoff stresses are equal to

$$P_i^{(lce)} = T_i^{(lce)} \lambda_i^{-1}, \quad i = 1, 2, 3. \tag{15}$$

Taking $\lambda_1 = \lambda$, we solve for λ_2 the equation

$$T_2^{(lce)} - T_3^{(lce)} = 0. \tag{16}$$

To capture the auxetic response while maintaining the continuum mechanics formulation tractable, we let the uniaxial scalar parameter $Q > 0$ decrease linearly with respect to the longitudinal stretch ratio λ from a given value $Q_0 \in (0, 1)$, at $\lambda = 1$, to a minimum value $Q_{crt} \in (0, Q_0)$ that occurs at the critical stretch ratio $\lambda = \lambda_{crt}$, then increase again, also linearly, to a value $Q_1 \in (Q_{crt}, Q_0)$, i.e.,

$$Q(\lambda) = \begin{cases} C_1 \lambda + D_1 & \text{for } 1 \leq \lambda \leq \lambda_{crt}, \\ C_2 \lambda + D_2 & \text{for } \lambda_{crt} \leq \lambda \leq \lambda_{max}, \end{cases} \tag{17}$$

such that $Q(1) = Q_0$, $Q(\lambda_{crt}) = Q_{crt}$ and $Q(\lambda_{max}) = Q_1$. Hence, $C_1 = (Q_0 - Q_{crt}) / (1 - \lambda_{crt})$, $D_1 = (Q_{crt} - \lambda_{crt} Q_0) / (1 - \lambda_{crt})$, $C_2 = (Q_{crt} - Q_1) / (\lambda_{crt} - \lambda_{max})$, $D_2 = (\lambda_{crt} Q_1 - \lambda_{max} Q_{crt}) / (\lambda_{crt} - \lambda_{max})$.

When a is given by (3) and $Q = Q(\lambda)$ is described by (17), the energy function is equal to

$$w(\lambda, \theta) = W^{(lce)}(\lambda_1, \lambda_2, \lambda_3, a, \theta), \tag{18}$$

where $W^{(lce)}(\lambda_1, \lambda_2, \lambda_3, a, \theta) = W^{(lce)}$ is defined by equation (1).

Solving the equation

$$w(\lambda, 0) = w(\lambda, \pi/2) \tag{19}$$

gives the critical stretch ratio $\lambda = \lambda_{crt}$.

3 Numerical example

To illustrate the mechanical behaviour predicted by the theoretical LCE model, in the numerical example, we set $n = 1$ and $m = -1$, and obtain:

- If $\theta = 0$, then

$$\lambda_2 = \lambda_2(\lambda, a) = \frac{1}{\sqrt{\lambda}} \left(\frac{\mu_1 + \mu_2 \lambda^2 a_0^{-2/3} a^{2/3}}{\mu_1 + \mu_2 \lambda^2 a_0^{1/3} a^{-1/3}} \right)^{1/4} \tag{20}$$

and

$$\lambda_3 = \frac{1}{\lambda_1 \lambda_2} = \frac{1}{\sqrt{\lambda}} \left(\frac{\mu_1 + \mu_2 \lambda^2 a_0^{1/3} a^{-1/3}}{\mu_1 + \mu_2 \lambda^2 a_0^{-2/3} a^{2/3}} \right)^{1/4}; \tag{21}$$

- If $\theta = \pi/2$, then

$$\lambda_2 = \lambda_2(\lambda, a) = \frac{1}{\sqrt{\lambda}} \left(\frac{\mu_1 + \mu_2 \lambda^2 a_0^{-2/3} a^{-1/3}}{\mu_1 + \mu_2 \lambda^2 a_0^{1/3} a^{-1/3}} \right)^{1/4} \tag{22}$$

Table 1 Cat skin experimental values for stretch ratio λ_3 in the thickness direction vs. stretch ratio λ_1 in the longitudinal direction [15]

λ_1	1.0000	1.2000	1.4000	1.5000	1.6000	1.7000	1.8000	1.8933	1.9400	2.0000	2.0667
λ_3	1.0000	1.0300	1.0500	1.0633	1.0833	1.1300	1.1533	1.1667	1.2033	1.2000	1.1833

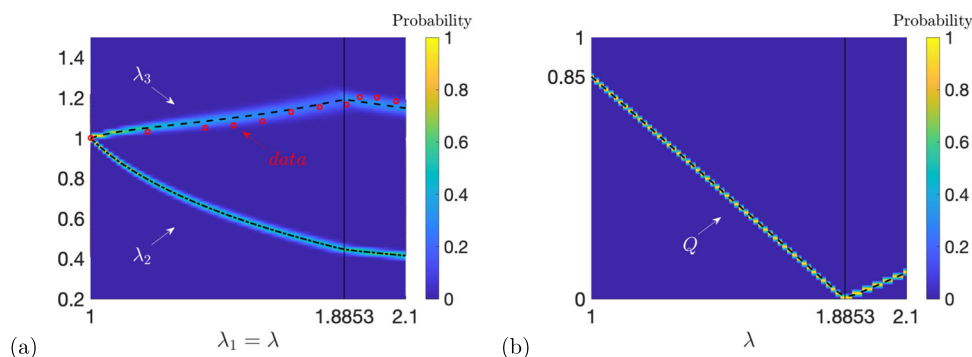


Fig. 1 (a) Computed transverse stretch ratio λ_2 and thickness stretch ratio λ_3 for the LCE model, and the associated experimental values for the deformation of cat skin under uniaxial tensile load, and (b) the scalar uniaxial order parameter Q , respectively. The vertical lines correspond to the predicted longitudinal stretch ratio $\lambda_1 = \lambda_{crit}$ where the director rotates suddenly. The dashed lines indicate mean values

and

$$\lambda_3 = \frac{1}{\lambda_1 \lambda_2} = \frac{1}{\sqrt{\lambda}} \left(\frac{\mu_1 + \mu_2 \lambda^2 a_0^{1/3} a^{-1/3}}{\mu_1 + \mu_2 \lambda^2 a_0^{-2/3} a^{-1/3}} \right)^{1/4} \tag{23}$$

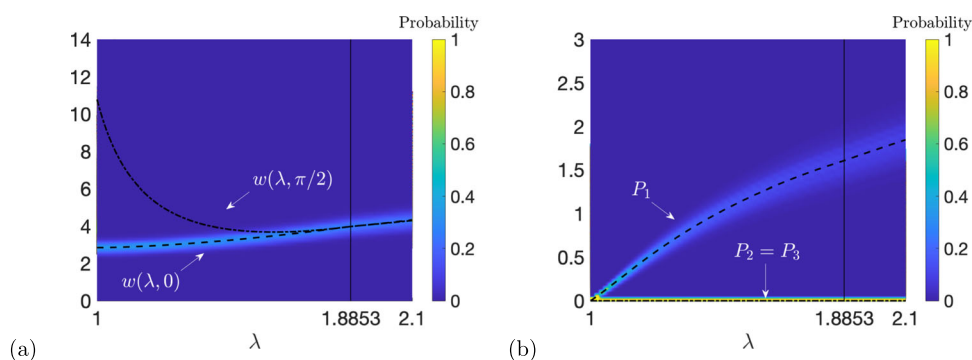
We further assume that μ follows a Gamma probability distribution with shape and scale parameters $\rho_1 = 190$ and $\rho_2 = 0.01$, respectively, while μ_1 follows a Beta distribution with hyperparameters $\xi_1 = 90$ and $\xi_2 = 100$. The mean values of the model parameters are then $\mu = \rho_1 \rho_2 = 1.9$, $\mu_1 = \mu \xi_1 / (\xi_1 + \xi_2) = 0.9$, and $\mu_2 = \mu - \mu_1 = 1$. These mean values were calibrated to the experimental data for cat skin displayed in Table 1. Note that, under the incompressibility assumption, which is valid for LCEs, and considered acceptable for cat skin in [15], $\lambda_2 = 1/(\lambda_1 \lambda_3)$. Therefore, the behaviour of λ_2 can be calculated from the data for λ_3 as a function of λ_1 . We also find $Q_0 = 0.85$, $Q_{crit} = 0.001$ and $Q_1 = 0.1$.

In Fig. 1(a), the auxetic response, showing how the stretch ratio corresponding to the thickness direction first increases then decreases, is captured. In the plots, as λ_3 records a change of monotonicity at $\lambda_1 = \lambda_{crit}$, a slight change in the gradient of λ_2 can also be observed, although this stretch ratio continues to decrease as λ_1 increases. Figure 1(b) depicts the associated deformation dependent uniaxial parameter Q given by equation (17). The energy function described by equation (18) is illustrated in Fig. 2(a). The corresponding first Piola-Kirchhoff stress defined by equation (15) is plotted in Fig. 2(b). The computer simulations were run in Matlab 2022a where inbuilt functions for random number generation were used.

4 Conclusion

Biomimetic materials are continuously sought in research fields such as biomedical engineering and regenerative medicine [1, 3]. This paper presents a hypothetical LCE model that mimics the unusual elastic response of cat skin examined experimentally and modelled within the theoretical framework of isotropic finite elasticity in [15]. Specifically, when a material sample is extended longitudinally, assuming that its volume is preserved, its thickness increases until a critical deformation is reached, then decreases. The hypothetical model suggests that LCEs could also be produced that exhibit

Fig. 2 (a) Energy function and (b) computed first Piola-Kirchhoff stress (in MPa), respectively. The vertical lines correspond to the predicted longitudinal stretch ratio $\lambda_1 = \lambda_{crit}$ where the director rotates suddenly. The dashed lines indicate mean values



such auxetic response, both under the small and large strain regimes. The present study may also reignite interest in the extraordinary mechanical behaviour of cat skin, which has been less investigated and discussed than other skin tissue types [4].

Appendix A: Stochastic model parameters

For the stochastic modelling of nematic LCEs adopted in this paper, the following hypotheses are required [5, Chapter 6]: For any given finite deformation, at any point in the material, the shear modulus $\mu > 0$ and its inverse, $1/\mu$, are second order random variables, i.e., they have finite mean value and finite variance. This assumption is guaranteed by setting the following mathematical expectations:

$$\begin{cases} E[\mu] = \underline{\mu} > 0, \\ E[\log \mu] = \nu, \text{ such that } |\nu| < +\infty. \end{cases} \tag{A.1}$$

The first constraint in (A.1) specifies the mean value for the random shear modulus μ , and the second constraint provides a condition from which it follows that $1/\mu$ is a second order random variable. By the maximum entropy principle, the shear modulus μ with mean value $\underline{\mu}$ and standard deviation $\|\mu\| = \sqrt{\text{Var}[\mu]}$ (which is equal to the square root of the variance, $\text{Var}[\mu]$) follows a Gamma probability distribution with shape and scale parameters $\rho_1 > 0$ and $\rho_2 > 0$, respectively, such that

$$\underline{\mu} = \rho_1 \rho_2, \quad \|\mu\| = \sqrt{\rho_1 \rho_2}. \tag{A.2}$$

The resulting probability density function takes the form

$$g(\mu; \rho_1, \rho_2) = \frac{\mu^{\rho_1-1} e^{-\mu/\rho_2}}{\rho_2^{\rho_1} \Gamma(\rho_1)}, \quad \text{for } \mu > 0 \text{ and } \rho_1, \rho_2 > 0, \tag{A.3}$$

where $\Gamma : \mathbb{R}_+^* \rightarrow \mathbb{R}$ is the complete Gamma function

$$\Gamma(z) = \int_0^{+\infty} t^{z-1} e^{-t} dt. \tag{A.4}$$

The word ‘hyperparameters’ is used for ρ_1 and ρ_2 to distinguish them from μ and other material constants.

When $\mu = \mu_1 + \mu_2$, assuming $\mu_i > 0, i = 1, 2$, we define the auxiliary random variable

$$R_1 = \frac{\mu_1}{\mu}, \tag{A.5}$$

such that $0 < R_1 < 1$. Then, the random model parameters can be expressed equivalently as follows,

$$\mu_1 = R_1 \mu, \quad \mu_2 = \mu - \mu_1 = (1 - R_1) \mu. \tag{A.6}$$

It is reasonable to assume

$$\begin{cases} E[\log R_1] = \nu_1, \text{ such that } |\nu_1| < +\infty, \\ E[\log(1 - R_1)] = \nu_2, \text{ such that } |\nu_2| < +\infty, \end{cases} \tag{A.7}$$

in which case, the random variable R_1 follows a standard Beta distribution, with hyperparameters $\xi_1 > 0$ and $\xi_2 > 0$ satisfying

$$\underline{R}_1 = \frac{\xi_1}{\xi_1 + \xi_2}, \quad \text{Var}[R_1] = \frac{\xi_1 \xi_2}{(\xi_1 + \xi_2)^2 (\xi_1 + \xi_2 + 1)}, \tag{A.8}$$

where \underline{R}_1 is the mean value and $\text{Var}[R_1]$ is the variance of R_1 . The associated probability density function is

$$\beta(r; \xi_1, \xi_2) = \frac{r^{\xi_1-1} (1-r)^{\xi_2-1}}{B(\xi_1, \xi_2)}, \quad \text{for } r \in (0, 1) \text{ and } \xi_1, \xi_2 > 0, \tag{A.9}$$

where $B : \mathbb{R}_+^* \times \mathbb{R}_+^* \rightarrow \mathbb{R}$ is the Beta function

$$B(x, y) = \int_0^1 t^{x-1} (1-t)^{y-1} dt. \tag{A.10}$$

For the random coefficients given by (A.6), the corresponding mean values are

$$\underline{\mu}_1 = \underline{R}_1 \underline{\mu}, \quad \underline{\mu}_2 = \underline{\mu} - \underline{\mu}_1 = (1 - \underline{R}_1) \underline{\mu}, \quad (\text{A.11})$$

and the variances and covariance take the form, respectively,

$$\text{Var}[\underline{\mu}_1] = (\underline{\mu} - 2b)^2 \text{Var}[R_1] + (\underline{R}_1)^2 \text{Var}[\underline{\mu}] + \text{Var}[\underline{\mu}] \text{Var}[R_1], \quad (\text{A.12})$$

$$\text{Var}[\underline{\mu}_2] = (\underline{\mu} - 2b)^2 \text{Var}[R_1] + (1 - \underline{R}_1)^2 \text{Var}[\underline{\mu}] + \text{Var}[\underline{\mu}] \text{Var}[R_1], \quad (\text{A.13})$$

$$\text{Cov}[\underline{\mu}_1, \underline{\mu}_2] = \frac{1}{2} (\text{Var}[\underline{\mu}] - \text{Var}[\underline{\mu}_1] - \text{Var}[\underline{\mu}_2]). \quad (\text{A.14})$$

Funding The support by the Engineering and Physical Sciences Research Council of Great Britain under research grant EP/S028870/1 to L. Angela Mihai is gratefully acknowledged.

Data Availability All data generated or analysed during this study are included in this article.

Declarations

Conflict of Interests The author has no competing interests to declare that are relevant to the content of this article.

Open Access This article is licensed under a Creative Commons Attribution 4.0 International License, which permits use, sharing, adaptation, distribution and reproduction in any medium or format, as long as you give appropriate credit to the original author(s) and the source, provide a link to the Creative Commons licence, and indicate if changes were made. The images or other third party material in this article are included in the article's Creative Commons licence, unless indicated otherwise in a credit line to the material. If material is not included in the article's Creative Commons licence and your intended use is not permitted by statutory regulation or exceeds the permitted use, you will need to obtain permission directly from the copyright holder. To view a copy of this licence, visit <http://creativecommons.org/licenses/by/4.0/>.

References

- Ambulo, C.P., Tasmin, S., Wang, S., Abdelrahman, M.K., Zimmern, P.E., Ware, T.H.: Processing advances in liquid crystal elastomers provide a path to biomedical applications. *J. Appl. Phys.* **128**, 140901 (2020). <https://doi.org/10.1063/5.0021143>
- de Gennes, P.G., Prost, J. *The physics of liquid crystals*, 2nd ed. Clarendon Press, Oxford (1993)
- Hussain, M., Jull, E.I.L., Mandle, R.J., Raistrick, T., Hine, P.J., Gleeson, H.F.: Liquid crystal elastomers for biological applications. *Nanomaterials* **11**, 813 (2021). <https://doi.org/10.3390/nano11030813>
- Joodaki, H., Panzer, M.P.: Skin mechanical properties and modeling: a review. *J. Eng. Med.* **232**(4), 323–343 (2018). <https://doi.org/10.1177/0954411918759801>
- Mihai, L.A.: Stochastic elasticity: a nondeterministic approach to the nonlinear field theory. Springer, Cham (2022). <https://doi.org/10.1007/978-3-031-06692-4>
- Mihai, L.A., Mistry, D., Raistrick, T., Gleeson, H.F., Goriely, A.: A mathematical model for the auxetic response of liquid crystal elastomers. *Philosophical Trans. R. Soc. A* **380**, 20210326 (2022). <https://doi.org/10.1098/rsta.2021.0326>
- Mihai, L.A., Raistrick, T., Gleeson, H.F., Mistry, D., Goriely, A.: A predictive theoretical model for stretch-induced instabilities in liquid crystal elastomers. *Liquid Crystals*. <https://doi.org/10.1080/02678292.2022.2161655> (2023)
- Mistry, D.: The richness of liquid crystal elastomer mechanics keeps growing. *Liq Cryst Today* **30**(4), 59–66 (2021). <https://doi.org/10.1080/1358314X.2022.2048974>
- Mistry, D., Connell, S.D., Mickthwaite, S.L., Morgan, P.B., Clamp, J.H., Gleeson, H.F.: Coincident molecular auxeticity and negative order parameter in a liquid crystal elastomer. *Nat. Commun.* **9**, 5095 (2018). <https://doi.org/10.1038/s41467-018-07587-y>
- Mistry, D., Gleeson, H.F.: Mechanical deformations of a liquid crystal elastomer at director angles between 0° and 90°: Deducing an empirical model encompassing anisotropic nonlinearity. *J. Polym. Sci.* **57**, 1367–1377 (2019). <https://doi.org/10.1002/polb.24879>
- Mistry, D., Nikkhou, M., Raistrick, T., Hussain, M., Jull, E.I.L., Baker, D.L., Gleeson, H.F.: Isotropic liquid crystal elastomers as exceptional photoelastic strain sensors. *Macromolecules* **53**, 3709–3718 (2020). <https://doi.org/10.1021/acs.macromol.9b02456>
- Raistrick, T., Zhang, Z., Mistry, D., Mattsson, J., Gleeson, H.F.: Understanding the physics of the auxetic response in a liquid crystal elastomer. *Phys. Rev. Res.* **3**, 023191 (2021). <https://doi.org/10.1103/PhysRevResearch.3.023191>
- Raistrick, T., Reynolds, M., Gleeson, H.F., Mattsson, J.: Influence of liquid crystallinity and mechanical deformation on the molecular relaxations of an auxetic liquid crystal elastomer. *Molecules* **26**, 7313 (2021). <https://doi.org/10.3390/molecules26237313>
- Truesdell, C., Noll, W. *The Non-Linear field theories of mechanics*, 3rd ed. Springer-Verlag, New York (2004)
- Veronda, D.R., Westmann, R.A.: Mechanical characterization of skin - finite deformations. *J. Biomech.* **3**(1), 111–124 (1970). [https://doi.org/10.1016/0021-9290\(70\)90055-2](https://doi.org/10.1016/0021-9290(70)90055-2)
- Vogel, S.: *Cat's paws and catapults*. WW norton and company, New York (1998)
- Warner, M., Terentjev, E.M.: *Liquid crystal elastomers*, paper back. Oxford University Press, Oxford (2007)

Publisher's note Springer Nature remains neutral with regard to jurisdictional claims in published maps and institutional affiliations.